IOP Publishing Measurement Science and Technology
Meas. Sci. Technol. **31** (2020) 055105 (8pp) https://doi.org/10.1088/1361-6501/ab6e24

Tetrahydroxyphenyl porphyrin membrane: a high-sensitivity optical waveguide gas sensor for NO_2 detection

Buayishamu Kutilike, Nuerguli Kari, Yuan Zhang, Patima Nizamidin and Abliz Yimit

College of Chemistry and Chemical Engineering, Xinjiang University, Ürümqi 830046, People's Republic of China

E-mail: ablizy@sina.com

Received 11 September 2019, revised 28 December 2019
Accepted for publication 21 January 2020
Published 5 March 2020

Abstract

In this study, 5,10,15,20-(4-hydroxyphenyl) porphyrin (THPP) was used as an optical waveguide (OWG) sensing material to detect several harmful acidic gases and volatile organic compounds. With this material, the sensor showed high selectivity and sensitivity to NO_2. First, a OWG sensor based on THPP was prepared using the spin-coating method. Next, the absorbance changes in the porphyrin film before and after interaction with NO_2 gas were analyzed using an ultraviolet-visible spectrophotometer. A 670 nm detection light source was selected for testing the OWG detection system; the optimum conditions were studied, where the lowest concentration detected by the sensor was 10 ppb. The film thickness (190 nm) was measured using scanning electron microscopy (SEM). Thereafter, the gas-sensing mechanism was further investigated through SEM, IR, and x-ray diffraction. Finally, the influence of ambient humidity on the sensor was analyzed. The results showed that ambient humidity can be neglected. The transducer exhibited uncomplicated fabrication and easy portability, and the detection process of OWG could be conducted at ambient temperature and resist electromagnetic interference.

Keywords: tetrahydroxyphenyl porphyrin film, NO_2 detection, OWG gas sensor, spin-coating method, porphyrin sensor

(Some figures may appear in colour only in the online journal)

1. Introduction

Nitrogen oxides are known for their adverse health effects on human respiratory organs. For example, they can react with water to produce nitrates, which when taken inside a human body, produce nitrite ammonia with strong carcinogens, so that less oxygen is available for the body to function properly. In addition, nitric acid is formed when NOx emitted from automobile exhaust enters the atmosphere and joins water vapor in the air, causing enough acid in the rainwater to create acid rain [1, 2]. The enormous and harmful impact of acid rain on human society and economy, as well as Earth's ecological environment, cannot be ignored. Nitrogen oxides are emitted, along with other harmful particulates, in the process of biomass gasification [3]. These said, controlling and detecting the content of noxious gases, such as NO_2, are urgent environmental issues that need to be addressed [4]. Various materials and methods of NO_2 detection seem to be in progress [5, 6], whereas presently, gas sensors are considered sensible and ideal as a substitute for measuring the amount of this gas in the environment [7]. The optical waveguide gas (OWG) sensor has been considered a better option than other existing ones because of its high sensitivity, fast response time, concise system, intrinsic safety detection and easy preparation, and good application prospect for gas detection [8, 9]. We recently experimented with the use of OWG sensors for detecting harmful gases such as amine [10], trimethylamine [11], hydrogen sulfide, and xylene at room temperature, and showed that the concentration of ppb level can be measured [12, 13]. Sensitive materials also play a decisive part in

 © 2020 IOP Publishing Ltd Printed in the UK

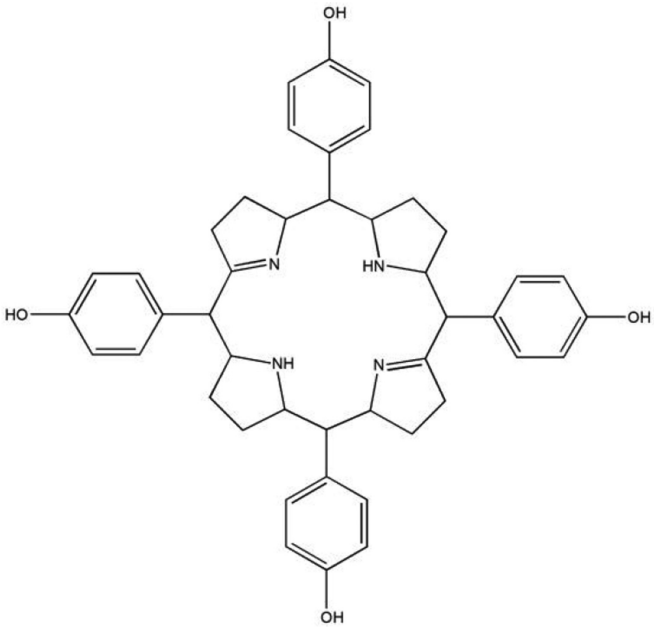

Figure 1. Structural diagram of THPP.

the gas-sensing measurement process of optical waveguides; thus, the selection of ideal sensitive materials is a key factor to be considered. A popular material and a candidate for sensor detection is porphyrin—capable of easy film formation, chemical stability, and coordination with various substances, as well as formation of different aggregates under acidic conditions [14].

Porphyrin molecules are macrocyclic compounds comprising four pyrrole rings linked by four methylenes [15]. They have a rich electron delocalization system, giving them unique optical, electronic, magnetic, redox, catalytic, and self-assembly properties [15]. Moreover, these molecules show strong absorption in the visible region and emission of more than 600 nano-wavelength in the fluorescence spectrum [16, 17]. In nature, porphyrins, in the form of metal complexes, exist in heme, chlorophyll, vitamin B12, and other living tissues, and participate in the transmission of oxygen and photosynthesis [18, 19]. These features and characterizations make them feasible as sensitive materials for detecting oxygen, volatile organic liquids, harmful inorganic gases, and excess metal ions [20]. In this study, we select tetrahydroxyphenyl porphyrin (THPP) as the sensitive material. THPP is fixed on the surface of a K^+-exchanged glass waveguide, as shown in figure 1, where the THPP thin film/K^+-exchanged glass waveguide sensor is developed for the detection of noxious gases.

2. Experimentation

2.1. Preparation of measured gas

To prepare the NO_2 gas, first, 22.4 mg of pure copper was weighed and placed into a 250 ml bottle. Next, a 0.1 ml concentrated nitric acid was injected into the bottle using a microsyringe. Once the reaction was complete, 1 ml NO_2 gas was extracted with a microsyringe and injected into a 600 ml standard volume container with NO_2 gas [21]. During this time, the NO_2 concentration was approximately 100 ppm [22], based on the readings on a commercial gas detection tube (note that the gas detector tube chemically reacted with the gas. The detector was dyed with a chemical reaction, and its dyeing length was directly proportional to the gas concentration. The concentration of the measured gas was evaluated from the printed scale on the detector tube (Gastec, Japan)). Subsequently, different concentrations of NO_2 gas were diluted with pure nitrogen in the second standard vessel (600 ml) to obtain the desired concentration. Through this standard container dilution method, a very low concentration of NO_2 (in ppb range) can be obtained [23, 24].

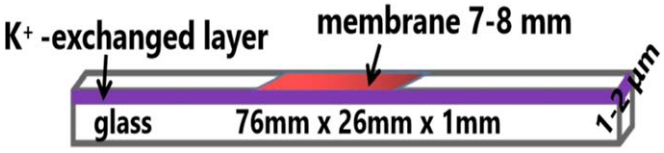

Figure 2. Schematic representation of the sensitive element.

To prepare a volatile organic compound vapor, a certain volume (trace) of the volatile organic compound (analytically pure) was injected into a standard volume container. The mixture was allowed to evaporate. The concentration was then confirmed with a gas detection tube and diluted with nitrogen to achieve the desired concentration.

2.2. Fabrication of sensitive elements

2.2.1. Preparation of K^+-exchanged glass OWG. A glass slide (76 mm × 26 mm × 1 mm) was immersed in molten KNO_3 salt at 400 °C for 40 min, as illustrated in figure 2, causing a change in the refractive index of the ion-exchange glass slide with that in the electronic polarizability of the metal ions [23]. Moreover, because the polarizability of potassium ion in neutral salt was much lower than that of sodium ion in the slide, potassium ion could be easily exchanged to the glass surface and formed a layer of potassium ion, as shown in equation (1), to improve the refractive index of the slide. The thickness of the waveguide layer formed by substitution of the sodium and potassium ions was 1–2 microns, while the refractive index increased from 1.510 to 1.518 [25]. After 40 min of immersion, the substrate (slide) was removed from the melted KNO_3, cooled under room temperature, and subsequently, washed with distilled water for removal of solid KNO_3 particles on its surface:

$$Na^+(\text{glass}) + K^+(\text{melt}) \rightarrow K^+(\text{glass}) + Na^+. \quad (1)$$

2.2.2. Preparation of THPP thin-film OWG sensing element. A certain amount of THPP powder was dissolved in 10 ml ethanol. The prepared THPP–ethanol solution was then coated on the surface of the K^+-exchanged glass OWG with a spin coater (the first rotation speed was 300 rpm for ~5 s, and the second rotation speed was 1400–2400 rpm for ~25 s). The solution

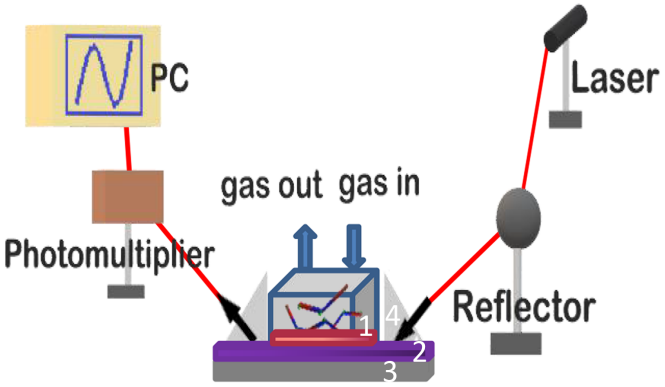

Figure 3. Optical waveguide detection system (1–sensitive film; 2–waveguide layer; 3–glass; 4–prism).

was finally dried under room temperature for 24 h prior to gas testing, as shown in figure 2.

2.3. Gas testing process

2.3.1. OWG system. Figure 3 shows the components of the OWG detection system, including a semiconductor laser, a reflector, a sensitive element, photomultiplier tubes, and a computer [26]. The semiconductor laser was allowed to pass through the K^+-exchanged glass-guided layer through the prism coupling method, and light was totally reflected in the guided wave layer and penetrated into the film surface in the form of an evanescent wave [27]. The optical absorption coefficient (α) of the sensitive film varied during the interaction between the measured gas and the sensitive layer. The intensity I of the emitted light in the optical waveguide sensor was determined as

$$I = I_0(1 - aNd_e) \tag{2}$$

where I_0 is the intensity of the incident light, a is the optical absorption coefficient, N is the surface reflectance number of the guided wave given length L, and d_e is the actual path length of light in the sensitive film. The actual thickness of the sensitive film, d_f, can be expressed as

$$N = L/(2d\tan\theta) \tag{3}$$

$$d_e = 2d_f/(\cos\theta). \tag{4}$$

Owing to the extreme sensitivity of the OWG sensor to the change in a, refractive index, and d_f of the film surface, when the sensitive film interacted with the measured gas, a small change in its optical properties (film thickness, absorbance, or transmittance) caused a significant change in the output light intensity [28].

2.3.2. Gas testing. The prepared THPP sensitive element was installed on the OWG detection system, and the guided light was excited through the prism coupling method. To allow the prism close to the glass waveguide, a diiodomethane liquid having a refractive index of 1.74 was dripped onto the interface. A semiconductor laser with 670 nm wavelength was input into the guided layer through the first prism, whereas the guided light was output from the second prism.

As the injected gas entered the interior, it assumed contact with the sensitive film, causing a change in the output light intensity. Meanwhile, the light signal output from the second prism was converted to electrical signals by the photomultiplier tube. Finally, the output light intensity was recorded through the computer (recorder).

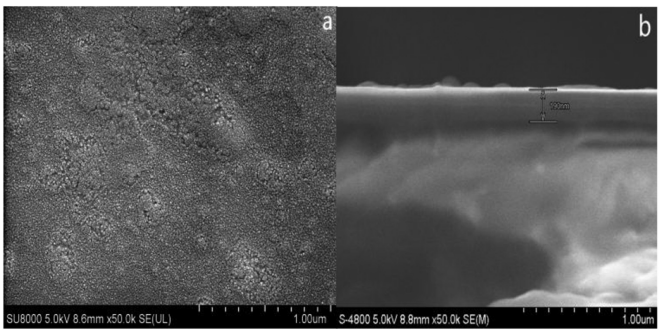

Figure 4. SEM images of the film membrane depicting its (a) surface morphology and (b) thickness.

3. Results and discussion

3.1. Scanning electron microscopy: morphological properties

The high sensitivity of gas sensors depends on the structure of the sensing materials. For instance, characteristics of large specific surface area, high porosity, and porous structure often play a vital role in improving the sensitivity of sensitive materials [29, 30]. The film's morphology and thickness were captured using SEM images, as displayed in figure 4. THPP was distributed in the form of uniform and dense particles on the glass surface, and its thickness was 190 nm. Note that the membrane thickness is a key factor in determining the material sensitivity [8].

3.2. Ultraviolet spectrum properties

When the THPP membrane assumed contact with the NO_2 gas, the UV–vis absorption spectra demonstrated corresponding changes in absorbance. In particular, a strong absorption peak of THPP at 434 nm was bathochromic-shifted to 26 nm, whereas the absorption peaks between 500 and 700 nm (Q peaks) were dissolved, paving way for the emergence of new absorption peaks at 688 nm. Considering the phenomena of laser intensity and astigmatism, a 670 nm laser was selected as an illuminant for the gas sensitivity test.

3.3. Gas-sensing performance of the THPP thin film

The working principle of the planar OWG sensor is based on changes in the optical properties (absorptivity, refractive index, or film thickness) of the sensitive layer when exposed to the detected gas. Here, a decrease or increase in absorbance gives rise to a change in the evanescent wave, where such a

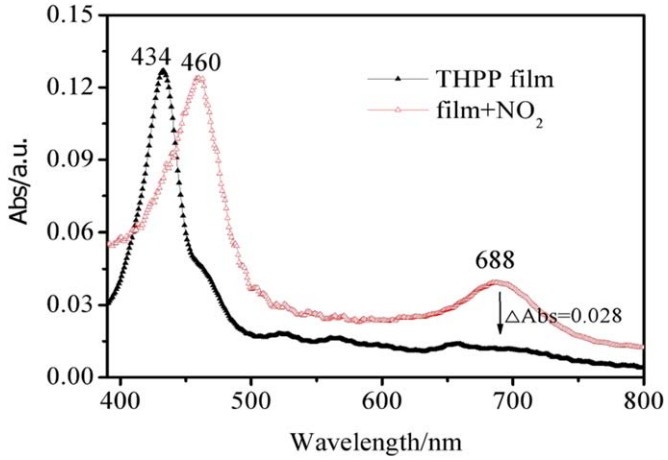

Figure 5. Absorption changes in NO_2 due to contact with THPP thin film.

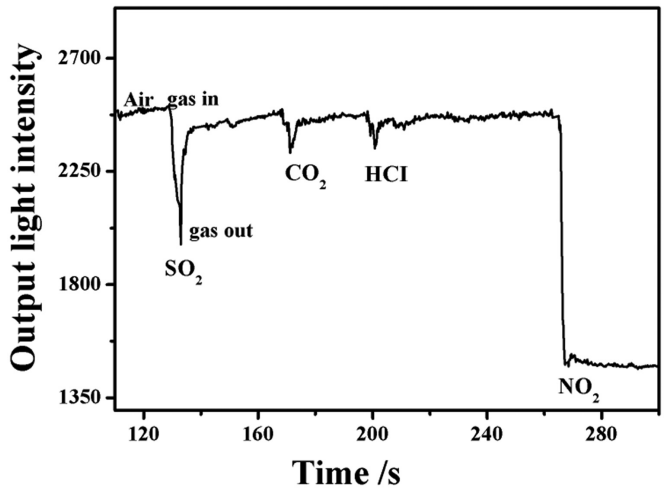

Figure 6. Response chart of OWG of acidic gas and sensitive element.

variation in the evanescent wave initiates a change in the output light intensity. In this study, the absorbance of the THPP film was observed to increase as soon as it came in contact with NO_2 at 688 nm, as depicted in figure 5. As such, the output light intensity decreased (as shown in figure 6) once the NO_2 gas was detected in the OWG detection system.

During the experiments, it was observed that when certain concentrations of NO_2, SO_2, CO_2, and HCl gases were injected into the OWG detection system, although the concentration of each gas was equal to 1000 ppm, the response to NO_2 was much greater than that to other gases (figure 6), with the output light intensity declining sharply without the baseline being restored. This confirms that the sensitive element exhibited certain selectivity to NO_2 gas.

In the preparation of sensitive elements, the speed of the coater and the concentration of the sensitive material solution are expected to impact the gas sensitivity of these elements. The membrane thickness depends on the rotation speed (a fast rotation speed is attributed to a thinner film, whereas a low speed is attributed to a thicker one). The absorption ability of light gets enhanced with the appropriate membrane thickness, causing the surface area and roughness to increase as well [26].

Here, it can be implied that increasing the thickness to a certain extent can effectively improve the film sensitivity. Meanwhile, concentration is a vital factor in determining the film thickness. In the experiments, the concentration of the THPP solution was varied at 0.001, 0.002, and 0.0005 mol l^{-1}, at corresponding coater rotation speeds of 1400, 1800, 2100, and 2400 rpm. Subsequently, the OWG sensitive elements were exposed to analyte gases (acidic gases and VOCs). The results showed a relatively high sensor response to each gas at 1800 rpm and 0.001 mol l^{-1} solution concentration. Thus, 1800 rpm and 0.001 mol l^{-1} were chosen as the optimum conditions, as illustrated in figures 7(a) and (b).

To study the correlation between the sensor and NO_2 concentration, the sensor element was re-fabricated under the optimum conditions mentioned above. Both were in contact at 10 ppm, 1 ppm, 100 ppb, and 10 ppb NO_2. As shown in the diagrams, when NO_2 had a minimum concentration of 10 ppb, the THPP/K^+-exchanged OWG element still exhibited NO_2 detection, thereby suggesting a good linear relation between the gas concentration and light intensity $R^2 = 0.9944$, as shown in figure 8.

Concerning the practical application of the sensor, the response and recovery time are also worth discussing. When the sensor was exposed to 1 ppm NO_2, the response and recovery time were 1 and 3 s, respectively, as shown in figure 9. With an increase in NO_2 concentration, the recovery time increased, and the high concentration did not restore the original baseline. Therefore, the sensor showed high sensitivity, stability (a set of experiments produced results showing that the response of the sensor after three months remained very high), and fast response and recovery time for NO_2 gas.

3.4. Gas-sensing mechanism

As illustrated in figure 10, the output light intensity of the THPP-sensing element decreased rapidly and did not recover after reaction with NO_2 (1000 ppm). When H_2S gas (1000 ppm) was applied to the sensor element injected with NO_2, the output light intensity was restored to its initial value (right), indicating that the substance formed after THPP assumed contact with NO_2 can be reduced by H_2S.

Figure 11(a) displays a micrograph SEM image of the THPP film, where particles on the surface of the thin film were uniformly and densely distributed, and had voids in between. Such a hole granular morphology could provide a fine channel for the electron transfer in the gas-sensing process [31, 32]. The film surface changed significantly into a uniform aggregation of particles into various shapes after exposure to NO_2, as shown in figure 11(b), which indicates a strong interaction between the film and NO_2. The agglomeration phenomenon in figure 11(b) disappeared completely in figure 11(c), i.e. when the THPP film that had interacted with NO_2 was in contact with H_2S again, and the film surface seemed to return to the pattern before contact with the gas figure 11(a). These results agree well with those shown in figure 10.

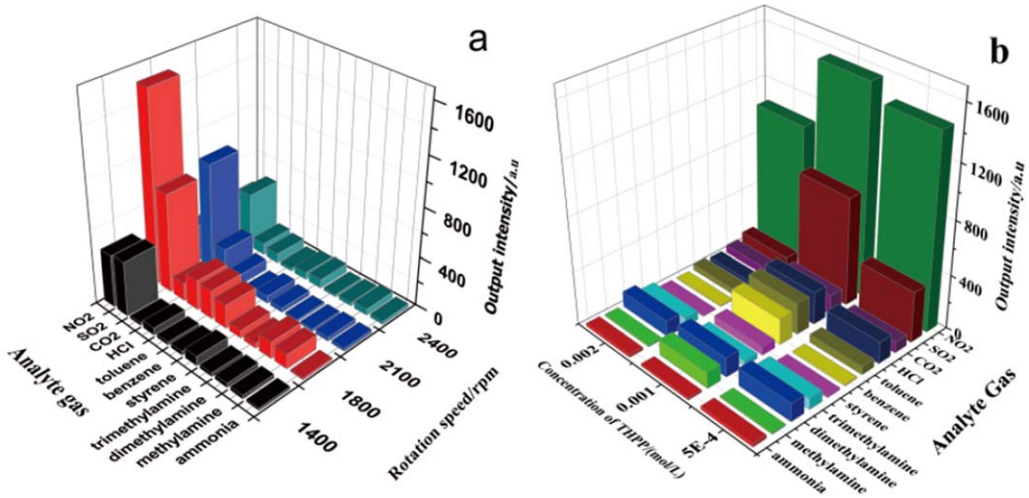

Figure 7. (a) Response of sensitive elements to different rotation velocities of analyte gases. (b) Detection results of sensitive elements prepared at different concentrations of the analyte gases.

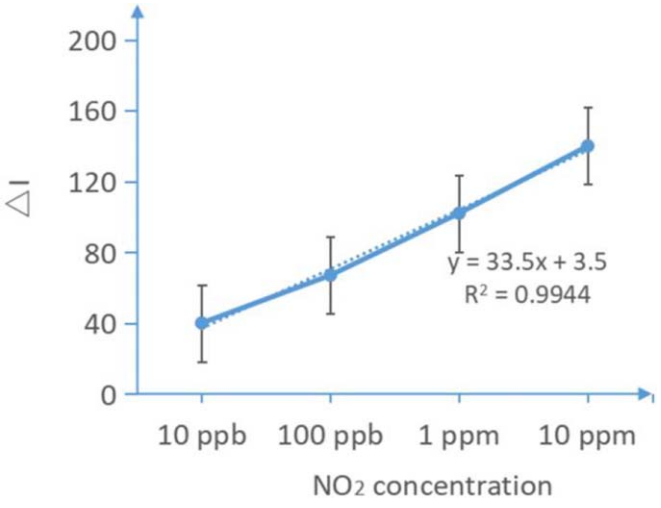

Figure 8. Linear relationship diagram of light intensity variation value of OWG element upon exposure to different concentration of NO_2.

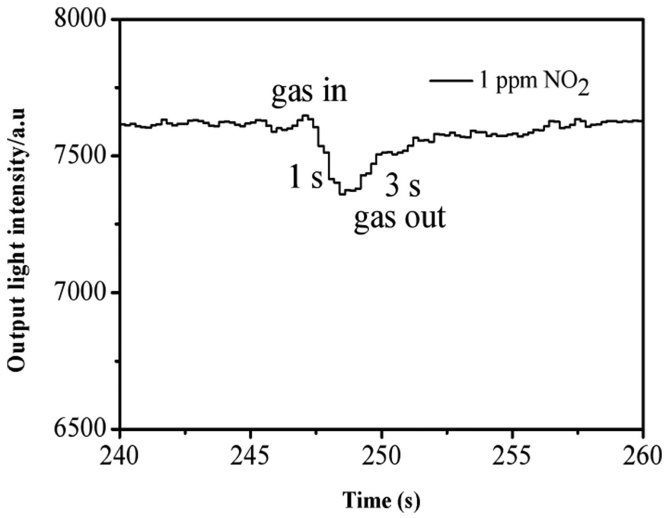

Figure 9. Typical response of THPP/K^+-exchanged OWG element to low concentrations of NO_2.

To verify these results, a Fourier transform infrared spectroscopy (FT-IR) test was conducted. Figure 12 displays the absorption curve of the film after contact with NO_2 and H_2S. In particular, figure 12(a) describes the IR absorption spectrum of the THPP film, figure 12(b) shows the film's IR spectrum after contact with NO_2, and figure 12(c) shows that of the sensitive membranes that first came in contact with NO_2 and then with H_2S. For the first curve, with N–H, the stretching vibration band of porphyrin was 3131 cm^{-1}, the bending vibration band was 965 cm^{-1}, and the out-of-plane sway absorption occurred at 734 cm^{-1} in the acromial form [33]. The absorption peaks at 1501–1640 cm^{-1} belonged to C = C on porphyrin rings, CH = N, and PhC–O at 1237 cm^{-1} [33, 34]. As the film came into contact with NO_2 [figure 12(b)], the change occurred at 1231–1290 and 1530 cm^{-1}. References [35, 36] assert that the bands at 1530 and 1290 cm^{-1} were in the form of bidentate nitric acid species (N = O) and (NO_3^-) [37, 38] (NO_3^- and NO were produced from the reaction of NO_2 with OH^- on porphyrin molecule [39], as shown in equation (5)). Most notable was the disappearance of the two peaks in figure 12(c) (the films were in contact with NO_2 and H_2S), indicating that when the THPP film (already exposed to NO_2) contacted H_2S, the N = O and nitrate products reacted with H_2S [40] (shown in equations (6) and (7)). Besides IR spectroscopy, x-ray diffraction measurements were also studied (the figure not given). The results demonstrated that when the sensitive membrane contacted the NO_2 gas, the intensity of the diffraction peak became stronger. On the contrary, when the film contacted H_2S, the intensity of the diffraction peak got weaker and coincided with the single film peak. These results are consistent with those shown in figure 10:

$$NO_2 + OH^- \rightarrow NO_3^- + H_2O + NO \quad (5)$$

$$NO + H_2S \rightarrow N_2O + H_2O + S \quad (6)$$

$$NO_3^- + H_2S \rightarrow N_2O + H_2O + S \quad (7)$$

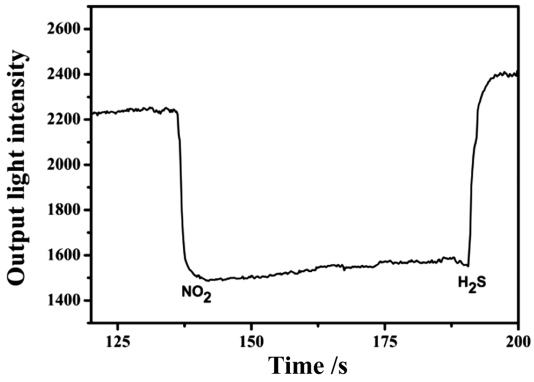

Figure 10. Response chart of sensitive thin film to NO_2 and H_2S on OWG system.

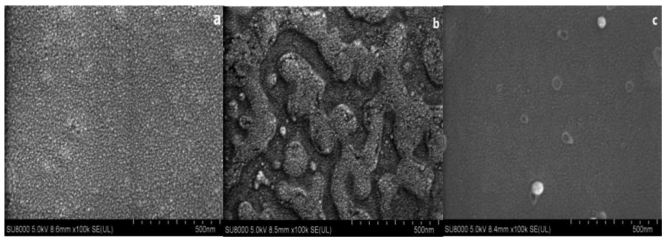

Figure 11. (a) SEM diagram of the film (b) after contact with the NO_2 gas and (c) subsequent contact with H_2S gas.

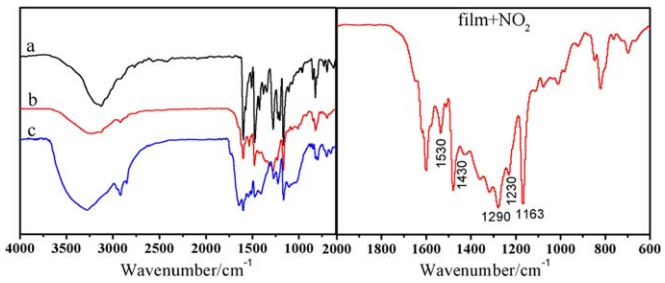

Figure 12. Infrared absorption spectrum curve of THPP film (a) after contact with NO_2 gas (b) after contact with H_2S gas again (c).

In conclusion, when the high-concentration NO_2 ($\geq$100 ppm) is in contact with the THPP film, the optical waveguide response does not recover, the film color changes from yellow to colorless, and the film surface is damaged (observed via SEM). The role between the THPP film and the NO_2 is a redox reaction. However, when the low-concentration NO_2 (below 100 ppm) is in contact with the film, the film color does not change, and the optical waveguide response also recovers, indicating that the interaction between porphyrin and NO_2 is reversible at this time. There are reports in the literature that this reaction exists between porphyrin and NO_2, and it is reversible [41, 42] (as shown in equation (8)). Hence, when the concentration of NO_2 varies, the interaction with the porphyrin molecule also varies:

$$\mathrm{THPP} + \mathrm{NO_2} \rightleftarrows \mathrm{THPP^+} \bullet + \mathrm{NO_2^-} \quad (8)$$

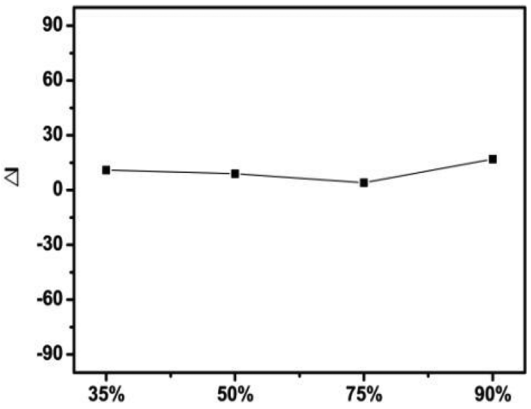

Figure 13. Influence of ambient humidity on the THPP sensitive film.

3.5. *Humidity influence testing*

To assess if there is any influence of ambient humidity on the gas sensitivity of the sensitive elements, the prepared sensor was installed on the OWG detection system and the response of the sensor to water vapor with different humidity values was detected. Set the ambient humidity to 35%, 50%, 75%, and 90% (humidity is prepared by evaporating different salt solutions ($MgCl_2$, NaCl, etc) and collecting evaporated water vapor). Contrary to this hypothesis, when the THPP/K^+-exchange OWG element is in contact with the different humidity, the output light intensity decreases, but the change is not great ($\Delta I = 14$), indicating that the humidity is within the range of 35%–90%, the sensor demonstrated an insignificant response to the different humidity values; thus, the influence of ambient humidity on the sensor was neglected during the experiment (as illustrated in figure 13).

4. Conclusion

In this study, THPP film/K^+-exchanged glass waveguide elements were prepared by mixing THPP with ethanol in three different concentrations and using a coater at different rotation speeds. The method was used to detect some noxious gases (NO_2, SO_2, CO_2, HCl, and VOCs) at room temperature. The sensitive elements exhibited fast response, high sensitivity, and selectivity to NO_2. Subsequently, the optimum conditions (solution concentration 0.001 mol l^{-1}, rotation speed 1800 rpm) were selected for the proposed OWG detection system. In the process, a distinct relation was found between the sensitive film and NO_2 (the output light intensity decreased rapidly and did not recover). Subsequently, the output light intensity of the sensitive film was restored to its original value after contact with H_2S. To further understand the phenomenon, SEM, FT-IR, and XRD images of the porphyrin films before and after interaction with NO_2 and H_2S were captured and analyzed. The results show that for high-concentration NO_2, the interaction with THPP is redox reaction. For low-concentration NO_2, the interaction

with THPP is reversible. Moreover, the minimum concentration of the sensor and the influence of the environmental humidity were also detected. The results showed that humidity does not significantly affect the sensor. The lowest detection concentration for NO_2 was 10 ppb, the value at which the sensor demonstrated characteristics of fast response and stability. For high-concentration NO_2 ($\geq$100 ppm), the sensitive film appeared colorless and could not be recovered. Therefore, in practical application, NO_2 gas with low concentration can be detected. Most NO_2 sensors can normally detect high concentrations, and this sensor compensate for the gap.

Acknowledgements

This work was supported by the National Natural Science Foundation of China (Grant No. 21765021) and Research and Innovation Project for graduate students in Xinjiang Uygur Autonomous Region (Grant No. XJGRI 2016011).

Conflicts of interest

There are no conflicts of interest to declare.

ORCID iDs

Buayishamu Kutilike https://orcid.org/0000-0003-1726-2632
Abliz Yimit https://orcid.org/0000-0001-6309-0064

References

[1] Zhang D *et al* 2012 Detection of NO_2 down to ppb levels using individual and multiple In_2O_3 nanowire devices *Nano Lett.* **4** 1919–24
[2] Cooney R V, Ross P D and Bartolini G L 1986 N-nitrosation and N-nitration of morpholine by nitrogen dioxide: inhibition by ascorbate, glutathione and alpha-tocopherol *Cancer Lett.* **32** 83–90
[3] Choi H I, Choi S W, Han C Y, Kim T-W, Kwon S-H, Moon H P, Roh K H and Wee N-S 2008 Two-dimensional offsets and medial axis transform *Adv. Comput. Math.* **28** 171–99
[4] Arshadi S and Anisheh F 2017 Theoretical study of Cr and Co-porphyrin-induced C70 fullerene: a request for a novel sensor of sulfur and nitrogen dioxide *J. Sulfur Chem.* **38** 1–15
[5] Hoffmann M W G *et al* 2014 Highly selective SAM–nanowire hybrid NO_2 sensor: insight into charge transfer dynamics and alignment of frontier molecular orbitals *Adv. Funct. Mater.* **24** 595–602
[6] Takao S *et al* 2010 Chemical and physical sensing by organic field-effect transistors and related devices *Adv. Mater.* **22** 3799–811
[7] Wetchakun K *et al* 2011 Semiconducting metal oxides as sensors for environmentally hazardous gases *Sens. Actuators* B **160** 580–91
[8] Yimit A *et al* 2005 Thin film composite optical waveguides for sensor applications: a review *Talanta* **65** 1102–9
[9] Giuliani J F, Wohltjen H and Jarvis N L 1983 Reversible optical waveguide sensor for ammonia vapors *Opt. Lett.* **8** 54–56
[10] Min Z *et al* 2017 Fabrication and gas sensing application of fast-responding m-CP-PVP composite film/potassium ion-exchanged glass optical waveguide *Anal. Methods* **9** 5494-501
[11] Turdi G *et al* A functionalized tetrakis(4-Nitrophenyl)porphyrin film optical waveguide sensor for detection of H_2S and ethanediamine gases *Sensors* **17** 2717
[12] Nizamidin P *et al* 2018 Characterization of the optical and gas sensitivities of a nickel-doped lithium iron phosphate thin film *Anal. Lett.* **51** 1–11
[13] Wang J *et al* 2018 Detection of trimethylamine based on a manganese tetraphenylporphyrin optical waveguide sensing element *Anal. Sci.* **34** 559–65
[14] Shinsuke I *et al* 2014 Porphyrin-based sensor nanoarchitectonics in diverse physical detection modes *Phys. Chem. Chem. Phys.* **16** 9713–46
[15] Shirsat M D *et al* 2012 Porphyrins-functionalized single-walled carbon nanotubes chemiresistive sensor arrays for VOCs *J. Phys. Chem. C Nanomater. Interfaces* **116** 3845–50
[16] Zhang C *et al* 2015 Porphyrin supramolecular 1D structures via surfactant-assisted self-assembly *Adv. Mater.* **27** 5379–87
[17] Yubin D *et al* 2015 Fluorescent and colorimetric ion probes based on conjugated oligopyrroles *Chem. Soc. Rev.* **44** 1101–12
[18] Lu G *et al* 2009 Tuning the morphology of self-assembled nanostructures of amphiphilic tetra(p-hydroxyphenyl)porphyrins with hydrogen bonding and metal–ligand coordination bonding *J. Mater. Chem.* **19** 2417–24
[19] Singin P V *et al* 2016 Simulation of porphyrin-ethanol solvate shell by DFT method. *J Porphyr Phthalocyanines* **19** 1212–8
[20] Yang J *et al* 2016 Real-time monitoring of dissolved oxygen with inherent oxygen-sensitive centers in metal-organic frameworks *Chem. Mater.* **28** 2652–8
[21] Hayrensa A *et al* 2008 Nafion film/K(+)-exchanged glass optical waveguide sensor for BTX detection *Anal. Chem.* **80** 7678–83
[22] Guanyun S *et al* 2000 Characteristic study of copper phthalocyanine as nitrogen dioxide gas sensitive material *Chem. Technol. Dev.* 38–39
[23] Yimit A, Itoh K and Murabayashi M 2003 Detection of ammonia in the ppt range based on a composite optical waveguide pH sensor *Sens. Actuators* B **88** 239–45
[24] Abdurahman R *et al* 2010 Optical waveguide sensor of volatile organic compounds based on PTA thin film *Anal. Chim. Acta* **658** 63–67
[25] Ablat H *et al* 2008 Nafion film/K(+)-exchanged glass optical waveguide sensor for BTX detection *Anal. Chem.* **80** 7678–83
[26] Abudukeremu H *et al* 2018 Highly sensitive free-base-porphyrin-based thin-film optical waveguide sensor for detection of low concentration NO_2 gas at ambient temperature *J. Mater. Sci.* **53** 1–13
[27] Turdi G *et al* 2016 Tetraphenylporphyrin film optical waveguide OWG sensor for detect volatile organic compounds gas. *Chin. J. Sens. Actuators* **29** 966–70
[28] Yimit A *et al* 2005 Thin film composite optical waveguides for sensor applications: a review *Talanta* **65** 1102–9
[29] Sun X *et al* 2014 A fluorescent polymer film with self-assembled three-dimensionally ordered nanopores: preparation, characterization and its application for explosives detection *J. Mater. Chem. A* **2** 14613–21
[30] Min H *et al* 2016 Sensitive and fast optical HCl gas sensor using a nanoporous fiber membrane consisting

of poly(lactic acid) doped with tetraphenylporphyrin *Microchimica Acta* **183** 1713–20
[31] Navale S T *et al* 2014 Highly selective and sensitive room temperature NO_2 gas sensor based on polypyrrole thin films *Synth. Met.* **189** 94–99
[32] Shi J T *et al* 2014 Two porous metal–organic frameworks (MOFs) based on mixed ligands: synthesis, structure and selective gas adsorption *Crystengcomm* **16** 3097–102
[33] Silverstein R M *et al* 1962 Spectrometric identification of organic compounds *J. Chem. Educ.* **39** 546–53
[34] Small G W 1992 Spectrometric identification of organic compounds *Vib. Spectrosc.* **4** 123–4
[35] Huang S J *et al* 2000 Adsorption and decomposition of NO on lanthanum oxide *J Catal* **192** 29–47
[36] Cayirtepe I *et al* 2009 Characterization of niobium-zirconium mixed oxide as a novel catalyst for selective catalytic reduction of NOx *Catalysis Letters* **132** 438
[37] Kantcheva M *et al* 2005 Characterization of LaMnAl 11 O 19 by FT-IR spectroscopy of adsorbed NO and NO/O_2 *Appl. Surf. Sci.* **252** 1481–91
[38] Peña D A *et al* 2004 Identification of surface species on titania-supported manganese, chromium, and copper oxide low-temperature SCR catalysts *J. Phys. Chem.* B **108** 9927–36
[39] Kantcheva M M, Bushev V P and Hadjiivanov K I 1993 ChemInform abstract: nitrogen dioxide adsorption on deuteroxylated titania (anatase) *Cheminform* **24** 25–25
[40] Ivanovic-Burmazovic I and Filipovic M R 2019 Saying NO to H_2S: a story of HNO, HSNO, and $SSNO^-$ *Inorg. Chem* **58** 4039−51 10.1021/acs.inorgchem.8b02592
[41] Peter C *et al* 2012 Metallo-porphyrin zinc as gas sensitive material for colorimetric gas sensors on planar optical waveguides *Microsyst. Technol.* **18** 925–30
[42] Shine H J, Padilla A G and Shi-Ming W 1979 ChemInform abstract: ion radicals. 45. Reactions of zinc tetraphenylporphyrin cation radical perchlorate with nucleophiles *Cheminform* **44** 4069–75